

## 2-Phenylimidazopyridines, a New Series of Golgi Compounds with Potent Antiviral Activity

Homayon Banie,<sup>†</sup> Anjana Sinha, Richard J. Thomas, Jagadish C. Sircar, and Mark L. Richards\*

Avanir Pharmaceuticals, 101 Enterprise, Aliso Viejo, California 92656

Received April 26, 2007

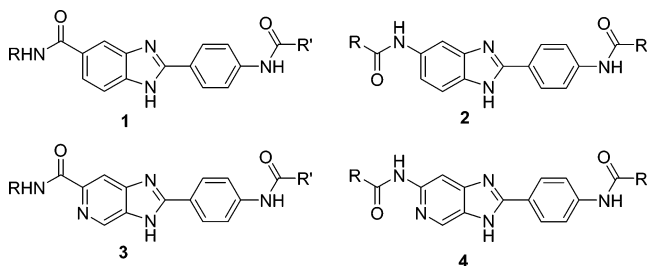
Drugs targeted to viral proteins are highly vulnerable to the development of resistant strains. We previously characterized a group of 2-phenylbenzimidazole compounds for their activity against allergy and asthma and more recently established the Golgi as their probable site of action. Herein we describe their activity against the propagation of several virus types through an action on the host cell. The most potent derivatives are the novel 2-phenylimidazopyridines, the lead compound of which is highly effective for blocking the spread of topical herpes infection in an animal model. These agents may provide an alternative antiviral approach, particularly for treating resistant strains.

### Introduction

The development of small molecule antiviral drugs has expanded in recent years primarily because of the success of HIV<sup>a</sup> (human immunodeficiency virus) drugs such as the protease and nucleosides reverse transcription inhibitors. However, viruses are innately efficient at developing resistance to these agents, thus requiring the use of drug combinations that target different viral proteins.<sup>1</sup> One largely unexplored approach to the treatment of viral diseases is the development of agents that target the host cell. Advantages of this strategy include a vastly expanded list of potential targets, a broader spectrum of activity, and less (theoretical) susceptibility to the development of resistance. Brefeldin A (BFA) is one such compound, disrupting Golgi function through inhibitory action on host cell ARF-1 GTPase.<sup>2</sup> A prominent disadvantage of targeting host cell proteins is a higher potential for toxicity, which for BFA is certainly the case. Nonetheless, the absolute dependence of virus on normal cellular functions and the wealth of unexplored host cell targets for treating viral diseases warrant further investigation of this approach.

We previously described a new class of 2-(substituted phenyl)benzimidazole (2-PB) drugs (**1** and **2**) that are effective in animal models of asthma, cancer, and inflammation.<sup>3–6</sup> Recent work has shown that these compounds act on the Golgi apparatus, resulting in a disruption of cisternae, displacement of resident Golgi proteins, and perturbation of oligosaccharide processing.<sup>7</sup> Because many viruses are known to utilize the Golgi of host cells during their life cycle, these compounds were tested for their ability to inhibit virus. We report that these agents inhibit the infectivity of viruses from several families that share a common need for host cell Golgi to envelop or move through the cell. In addition, a novel group of imidazopyridine derivatives (**3** and **4**) of the 2-PB backbone are described that share many characteristics with the corresponding 2-PB compounds but with a higher relative potency for inhibiting virus. The most

potent imidazopyridine derivative, *N*-(4-(6-adamantanecarboxamido)-3*H*-imidazo[4,5-*c*]pyridin-2-yl)phenyladamantanecarboxamide (**4a**) is shown to be highly effective at aborting the development of vesicles in a guinea pig model of herpes infection.



### Chemistry

Synthesis of the 2-phenylbenzimidazole compounds (Series **1**, **2**) have been described.<sup>3,4</sup> Series **3** and **4** compounds are depicted in Schemes 1 and 2, respectively.

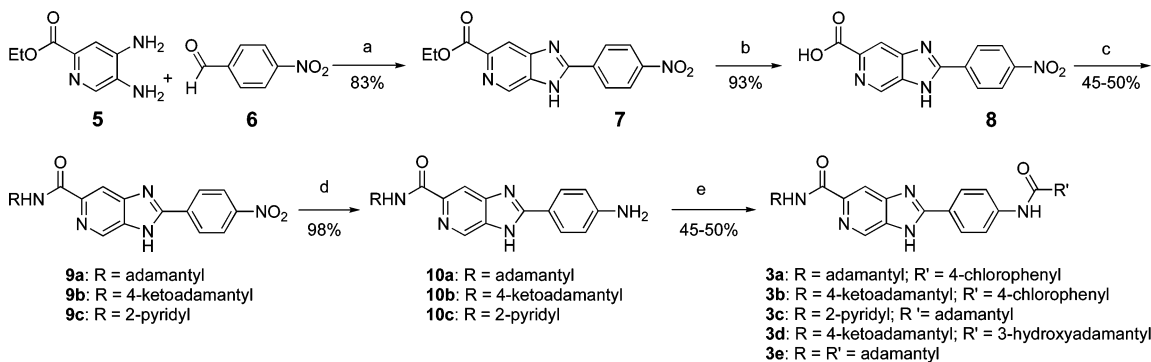
In one method (Scheme 1), 4-aminopicolinic acid was prepared by catalytic hydrogenation of commercially available picloram methyl ester (Sigma-Aldrich, St Louis, MO) and used as the starting material. Simultaneous nitration and rearrangement of 4-aminopicolinic acid by concd H<sub>2</sub>SO<sub>4</sub> and potassium nitrate followed with esterification of the carboxylic acid group gave ethyl 4-amino-5-nitropyridine-1-carboxylate. Catalytic hydrogenation of the latter over palladium on carbon in 2-propanol resulted in ethyl 4,5-diaminopyridine-2-carboxylate (**5**). The diamine **5** was coupled to 4-nitrobenzaldehyde (**6**) in nitrobenzene at 200 °C to give ethyl 2-(4-nitrophenyl)-3*H*-imidazo[4,5-*c*]pyridine-6-carboxylate (**7**) as a brown solid. Hydrolysis of the ethyl ester of **7** with 10% ethanolic NaOH at reflux gave 2-(4-nitrophenyl)-3*H*-imidazo[4,5-*c*]pyridine-6-carboxylic acid (**8**). Coupling of the free acid **8** to the appropriate alkyl or aliphatic amines with CDI in DMF afforded the nitro amide **9**. The nitro group in **9** was reduced to the corresponding amine of **10** and finally coupled with an appropriate acid chloride to yield the final compounds of this series **3a** to **3e**.

In another method (Scheme 2), the diamino backbone (**13**) was prepared from 2-(4-nitrophenyl)-3*H*-imidazo[4,5-*c*]pyridine-6-carboxylic acid (**8**). Curtius reaction of the acid **8** with DPPA, Et<sub>3</sub>N, and *t*-BuOH using NMP as a solvent afforded the nitro carbamate **11**. This carbamate was subjected to nitro group

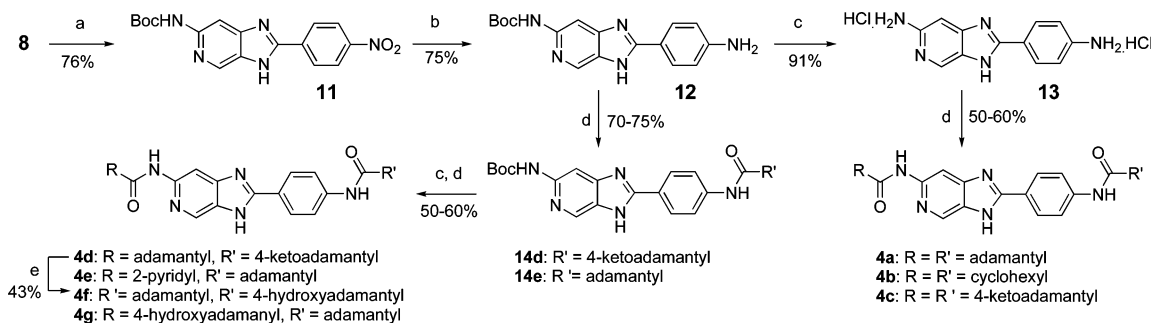
\* To whom correspondence should be addressed. Phone: (858) 414-1821. Fax: (949) 643-6815. E-mail: markrichards@yahoo.com.

<sup>†</sup> Current address: Department of Immunology, Johnson and Johnson Pharmaceutical Research and Development, 3210 Merryfield Row, San Diego, CA 92121.

<sup>a</sup> Abbreviations: 2-PB, 2-(substituted phenyl)benzimidazole; 2-PIP, 2-(substituted phenyl)imidazopyridine; HIV, human immunodeficiency virus; ERGIC, endoplasmic reticulum-Golgi intermediate compartment; BFA, brefeldin A; MOI, multiplicity of infection; PFU, plaque-forming units; HSV, herpes simplex virus; VSV, vesicular stomatitis virus; MHV, mouse hepatitis virus; VZV, varicella zoster virus; SV40, simian virus 40.

Scheme 1<sup>a</sup>

<sup>a</sup> Key: (a) Nitrobenzene, 200 °C, 18h; (b) 10% NaOH, EtOH, 90 °C, 1 h, 3 N HCl; (c) RNH<sub>2</sub>, CDI or PyBop, DMF, RT or 100 °C, 16 h; (d) Raney nickel, MeOH–THF–DMF, H<sub>2</sub>, 85 °C, 2 h; (e) (i) R'COCl, Py, RT, 4 h; (ii) 10% NaOH, EtOH, RT, 1 h.

Scheme 2<sup>a</sup>

<sup>a</sup> Key: (a) NMP, DPPA, Et<sub>3</sub>N, *tert*-BuOH, 85 °C, 6 h; (b) 10% Pd/C, NMP, 45 °C, 12 h; (c) HCl, dioxane, 90 °C, 1 h; (d) (i) RCOCN or R'COCl, Py, 120 °C, 3 h; (ii) 10% NaOH, EtOH, RT, 1 h; (e) NaBH<sub>4</sub>, EtOH, 90 °C, 1 h.

reduction with palladium on carbon in a Parr shaker to afford amine **12**. The amine carbamate **12** was hydrolyzed with acid to afford the diamine salt **13** which was coupled with the appropriate acid chlorides at 120 °C to afford the bisamides **4a–c**. For the nonsymmetrical bisamides **4d–g**, the amine **12** was coupled with appropriate acid chlorides to afford the amide carbamates **14d,e**. The carbamate group in **14** was hydrolyzed to the corresponding amine and subsequently coupled with appropriate acid chlorides in pyridine at 120 °C to afford the unsymmetrical diamides **4d–g**.

**General Methods.** All reactions were carried out under an inert argon atmosphere with dry solvents under anhydrous conditions unless otherwise stated. All dried solvents (THF, DMF, DCM, NMP, MeOH, pyridine, Et<sub>3</sub>N) and reagents were purchased at the highest commercial quality from Aldrich and used without further purification. Reactions were monitored by thin layer chromatography (TLC) carried out on 0.25 mm E. Merck silica gel plates (60F-254) using UV light ( $\lambda_{\max}$  = 254) for visualization and an acidic mixture of *p*-anisaldehyde and phosphomolybdic acid and heat as the developing agents. E. Merck silica gel (60, particle size 0.043–0.063 mm) was used for flash column chromatography. NMR spectra were recorded on Bruker DRX-400 instruments and calibrated using residual undeuterated solvent as an internal reference. The following abbreviations (or combinations thereof) were used to explain the multiplicities: s = singlet, d = doublet, t = triplet, q = quartet, m = multiplet, br = broad. Low-resolution mass spectra were recorded on an Agilent LC/MS system.

## Biological Methods

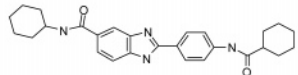
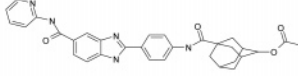
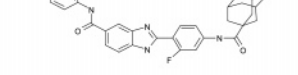
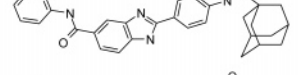
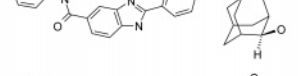
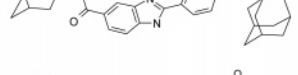
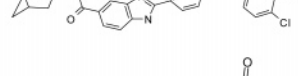
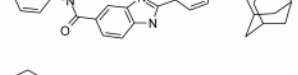
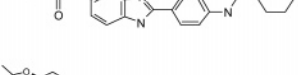
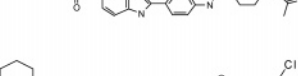
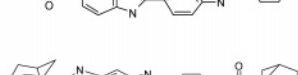
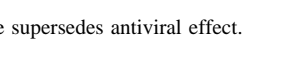
**General Approach.** To determine the specificity of their antiviral effect, 2-PB compounds were tested against the

propagation of nine viruses representing eight distinct viral families. Antiviral potency was compared to their potency for inhibiting IgE in vitro. New derivatives of these 2-PB compounds were also synthesized and tested, resulting in the identification of 2-phenylimidazopyridines (2-PIP) as the most potent antiviral analogues. One of the latter agents **4a** was tested for its ability to prevent vesicular eruption in a guinea pig model of topical herpes infection.

**Reagents.** All cell lines and viruses were obtained from ATCC. Vero, HeLa, and HeLa-H1 cells were cultured in MEM media (Gibco); NCTC clone 1469 was cultured in high glucose DMEM media (Gibco). Media formulations contained 10% FBS (Omega Scientific, Tarzana, CA), 2 mM L-glutamine and 1% penicillin-streptomycin solution (final 50 units/mL and 50 µg/mL, respectively) (Gibco), and maintained at 37 °C in a 10% CO<sub>2</sub> (DMEM and MEM) or 5% CO<sub>2</sub> (RPMI) atmosphere. Female hairless IAF/HA-HO guinea pigs were purchased from Charles River (Wilmington, MA). Murine recombinant IL-4 was obtained from PeproTech, Inc. (Rocky Hill, NJ). Anti-mouse CD40 antibody was obtained from BD-Pharmingen (San Jose, CA). Polyclonal goat antibodies against mouse IgE were prepared in-house as described.<sup>8</sup> Horseradish peroxidase-labeled anti-goat antibody was obtained from Santa Cruz Biotechnology, Inc.

**IgE Response.** This assay is described in detail in a previous report.<sup>3</sup> Briefly, spleen cells were isolated from naïve female BALB/c mice and cultured for 4 days in the presence or absence of IL-4 (10 ng/mL) and anti-CD40 antibody (100 ng/mL). ELISA plates were prepared by coating with 1 µg/mL goat anti-mouse IgE overnight followed by an overnight incubation with the 4-day culture supernatants at 4 °C. IgE was quantified following successive 90 min incubations with biotinylated goat

**Table 1.** Structure and Antiviral Activity of 2-Phenylbenzimidazoles<sup>a</sup>

Compound	IC50 (nM)									
	IgE	HSV-2	Vaccinia	VSV	MHV	California Encephalitis	San Angelo	Modoc	Rhino	SV40
<b>1a</b> 	70	2000	2000	>2000	20	35	130	>600*	600*	>2000
<b>1b</b> 	10	1000	1500	>2000	>600*	130	60	200	200	>2000
<b>1c</b> 	10	150	600	>2000	60	200	200	60	400	>2000
<b>1d</b> 	12	300	300	>2000	30	200	200	60	200	>2000
<b>1e</b> 	10	1500	1800	>2000	100*	60	135	400*	200	>2000
<b>1f</b> 	5	40	600	>2000	20	60	20	60	20	>2000
<b>1g</b> 	1	20	20	>2000	8*	20	6	6*	20*	>2000
<b>1h</b> 	4	30	40	>2000	20	60	20	60	20	>2000
<b>2a</b> 	5	170	200	1000	200	200	200	50	160	1000
<b>2b</b> 	1000	>2000	>2000	1000	>600*	>2000	>2000	>600*	>2000	1500
<b>2c</b> 	3	60	600	>2000	20	200	60	20	200	>2000
<b>2d</b> 	1	20	400	>2000	12	30	60	20	60	1200

<sup>a</sup> Antiproliferative supersedes antiviral effect.

anti-mouse IgE, alkaline phosphatase-streptavidin (Zymed, Carlsbad, CA), and 100  $\mu$ L of phenolphthalein monophosphate, DCHA salt (40 mg/mL). Absorption was measured at 540 $\lambda$ .

**Viral Propagation.** Cells were seeded at approximately 50 000/well in 24-well polystyrene plates. After 24 h fresh media was added without or with virus at a multiplicity of infection (MOI) of 0.1 or less, along with drug. Vero cells were infected with herpes simplex virus (HSV), vaccinia, vesicular stomatitis virus (VSV), California encephalitis, San Angelo, or Simian virus 40 (SV40). Mouse hepatitis virus (MHV) was grown in NCTC clone-1469 cells, and Modoc and Rhino viruses were grown in HeLa-H1 cells. When viral infectivity became evident, cells were washed and stained (1 g of methylene blue, 0.5 g of carbol fushin, 400 mL of methanol) for 10 min at room temperature. For plaque-forming viruses (HSV, vaccinia, Modoc, California Encephalitis, San Angelo, VSV, and Rhino), visual enumeration of clear zones on the culture plates was used

to estimate virus spread. MHV infectivity was visually estimated from the prevalence of clumped or lysed cells. SV40 infectivity was assessed by syncytia formation.

**In Vivo HSV-2 Model.** Female hairless IAF/HA-HO guinea pigs were anesthetized with isoflurane (Abbott Laboratories, North Chicago, IL) and inoculated with 1 million plaque forming units (PFU) of HSV-2 (MS strain) with a tattoo marker (Spaulding and Rogers Inc., Voorheesville, NY). Each guinea pig was inoculated with virus at three sites on the back, and the treatment modality was rotated between each of the sites. Drug treatment was initiated 24 h after inoculation by applying 50  $\mu$ L of vehicle/drug and continued four times per day at about 2.5 h intervals. Results were assessed on day 4 following inoculation. Delivery of **4a** was accomplished in a vehicle consisting of 38% Gelucire 44/14, (Gattefossé, Cedex, France), 38% polyethylene glycol 400, 10% tween 80, and 10% 1-methyl-2-pyrrolidinone (Sigma-Aldrich).

## Results and Discussion

Using a proteomic approach, we previously localized the molecular activity of 2-PB compounds to a group of proteins that function within the Golgi, whereas proteins of other organelles involved in synthesis, processing, and transport are apparently left unperturbed.<sup>7</sup> The affected proteins normally move in an anterograde fashion co-incident with the natural process of Golgi maturation and recycled back to proximal Golgi membranes by coatamer-coated vesicles known as COPI.<sup>9</sup> In cells exposed to 2-PB compounds, there is a defect in the recycling of these proteins from the distal membranes (trans-Golgi or trans-Golgi network) to the proximal membranes of the Golgi apparatus, resulting in the displacement of these proteins from the juxtannuclear region. This is normally followed by their degradation in the proteasome or lysosome,<sup>7</sup> although in resistant cancer cells these proteins are not degraded.<sup>5</sup> Moreover, co-incident with the displacement of these proteins is a change in the morphology of Golgi cisternae and a protein glycosylation defect that gives rise to EndoH sensitivity thus further implicating enzymes localized to the Golgi.<sup>7</sup> Finally, these actions are observed following exposure to the same drug concentrations that give rise to suppression of cytokine and IgE responses.

The impact of these agents on the Golgi of eukaryotic cells would suggest that they may affect the propagation of certain viruses that employ the Golgi for their intracellular maturation. Viruses exhibit multiple structure types, encode a diverse array of proteins, and employ a variety of mechanisms to reproduce and spread from cell to cell. To aid its packaging, lipid envelopment, and transportation through the host cell, viruses utilize many cellular proteins and organelles. Many viruses appear to rely on the Golgi apparatus, for example, to contribute membrane for lipid envelopment or to participate in the processing of critical viral proteins. Because 2-PB compounds cause dysfunctions in protein and presumably lipid processing events,<sup>7</sup> the activity of these agents was tested against virus.

Selected 2-PB compounds were tested for their effect on nine viruses representing eight different families (Table 1). Four different cell lines were used to grow virus in vitro. Compounds chosen for testing represent a cross-section of the agents previously tested for their activity against IgE<sup>3,4</sup> including compounds previously shown to be effective in models of allergy (**1d**) and cancer (**2a**, **1c**). Of the 11 viruses tested, 9 (HSV-1, HSV-2, VZV, vaccinia, MHV, California Encephalitis, San Angelo, Modoc, and Rhino) were highly susceptible to the action of 2-PB drugs while 2 (VSV and SV40) showed substantial resistance. Not shown are the results with HSV-1 or VZV of the *Herpesviridae*, which paralleled the results with HSV-2 (data not shown).

With the exception of Rhinovirus of the *Picornaviridae* family, viruses susceptible to the action of these compounds have been reported to use membranes of the Golgi, a pre-Golgi compartment known as the ERGIC (endoplasmic reticulum-Golgi intermediate compartment), or the trans-Golgi network for their envelopment.<sup>10</sup> Rhinovirus on the other hand, are nonenveloped and thus do not require lipid. They do however pass through the ERGIC during their life cycle and have been reported to perturb Golgi function.<sup>11</sup> Thus, all of the susceptible viruses are linked by their requirement for a functioning Golgi. These viruses are members of virus families that include important human pathogens such as *Bunyaviridae* (e.g., California Encephalitis, San Angelo, Hanta), *Coronaviridae* (e.g., SARS), *Flaviviridae* (e.g., Modoc, Hepatitis C, West Nile), *Herpesviridae* (e.g., HSV-1, HSV-2, VZV), *Poxviridae* (e.g.,

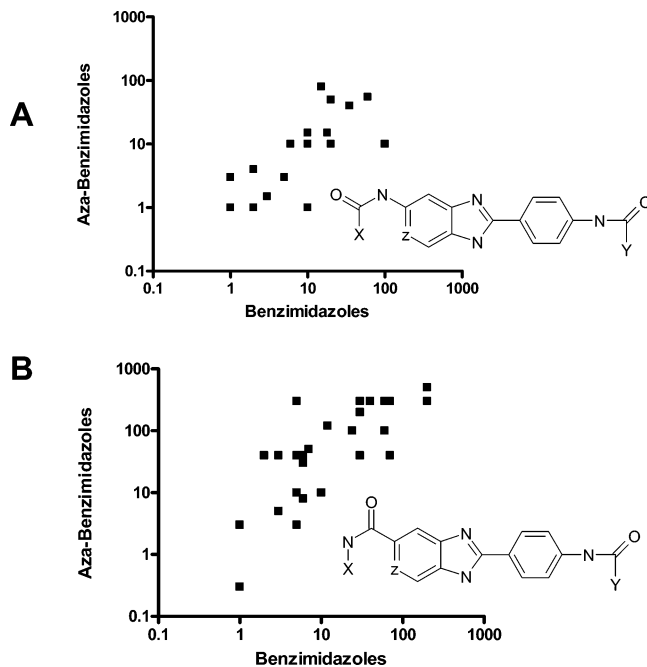


**Figure 1.** The  $IC_{50}$  of a series of paired 2-PB and 2-PIP compounds against IgE response in vitro are plotted. Each data point plots the  $IC_{50}$  of a benzimidazole (2-PB) and aza-derivative (2-PIP), which differ only in the “Z” position (C or N, respectively). A.  $IC_{50}$ s for analogues having the OC–N–N–CO amide linkage are plotted. The mean  $IC_{50}$  values for 2-PB and aza-derivative (2-PIP) compounds are 19 nM and 18 nM, respectively. B.  $IC_{50}$ s for analogues having the N–CO–N–CO amide linkage are plotted. Mean values for 2-PB and 2-PIP compounds are 29 nM and 180 nM, respectively. Two-tailed comparison showed a significant correlation between the  $IC_{50}$ s for the paired 2-PB and 2-PIP compounds ( $P < 0.0002$ ).

vaccinia, Small Pox) and *Picornaviridae* (e.g., Rhinovirus, Polio). Moreover, because they act on the Golgi, these compounds may inhibit viruses from other families known to rely on this organelle, including viruses from *Arenaviridae* (e.g., Lassa), *Calciviridae* (e.g., Norwalk), *Filoviridae* (e.g., Ebola), *Hepadnaviridae* (e.g., Hepatitis B), *Retroviridae* (e.g., HIV), and *Togaviridae* (e.g., rubella).

Viruses that are not affected by these drugs include SV40 (*Papovaviridae*) and VSV (*Rhabdoviridae*). While the G protein of the lipid enveloped VSV is glycosylated within the Golgi,<sup>12</sup> its processing has not been reported to be critical for function. SV40 is nonenveloped, and there have been no reports linking any critical Golgi processing events for this virus.<sup>13</sup> Interestingly, another compound known to inhibit Golgi function, BFA, has been reported to block SV40 infectivity.<sup>14</sup> However this action of BFA is mediated by perturbation of the caveosome, a non-Golgi organelle important for the life cycle of SV40. These results differentiate the action of BFA from 2-PB compounds, confirm the putative site of activity of these agents, and further underline the importance of the Golgi for the infectivity of many important viral pathogens.

While testing new analogues of the 2-PB compounds, a group of 2-phenylimidazopyridine derivatives (2-PIP) with a high potency for suppressing IgE response were identified. A number of analogues of the 2-PIP compounds were then synthesized and tested for IgE suppression, revealing a close parallel with the potency of 2-PB compounds. Because of their greater potential as therapeutic agents, only two of the four series of benzimidazole compounds<sup>4</sup> are compared. When orienting the amide linkages flanking the imidazole core as mirror images

Table 2. Structure and Antiviral Activity of 2-Phenylimidazopyridines<sup>a</sup>

Compound	IC <sub>50</sub> (nM)										
	IgE	HSV-2	Vaccinia	VSV	MHV	California Encephalitis	San Angelo	Modoc	Rhino	SV40	
3a		3	20	40	>2000	60	60	20	20	400	>2000
3b		0.15	40	40	1000	100*	200	135	>600*	20	>2000
3c		120	600	1500	>2000	50	40	40	600	200	>2000
3d		140	>2000	>2000	>2000	>600*	200	200	>600*	100	>2000
3e		10	30	140	>2000	20	60	60	100*	40	>2000
4a		1	5	10	>2000	8	6	6	20*	10	>2000
4b		1.5	20	60	>2000	15	60	20	6	60	>2000
4c		45	>2000	>2000	>2000	>600*	200	200	>600	>2000	1000
4d		4	250	400	>2000	200	200	200	>600*	>2000	>2000
4e		10	75	500	1000	60	60	60	60	60	>2000
4f		1	60	120	1000	20	200	60	20	10	>2000
4g		0.15	90	400	>2000	200	60	60	20	20*	1000

<sup>a</sup> Antiproliferative supersedes antiviral effect.

(OC–N – N–CO; series **2** and **4**), a comparable inhibition of IgE results for the corresponding 2-PB and 2-PIP analogues (Figure 1A). A similar comparison wherein the amides are in tandem (N–CO–N–CO; series **1** and **3**), however, results in a steeper curve indicating that the comparable 2-PIP compounds are of lower potency than the 2-PB analogues (Figure 1B). This loss of activity probably results from an interaction between the aza nitrogen with the amide. Thus with the caveat that the series **3** 2-PIP agents have lower relative potency than the corresponding series **1** 2-PB compounds, the SAR previously developed for IgE suppression by the 2-PB compounds<sup>4</sup> applies to the new 2-PIP agents.

Table 2 shows the antiviral activity of selected 2-PIP compounds, which for the most part also follows the pattern observed with the 2-PB compounds in Table 1. Indeed, a comparison of the activity of the 24 compounds listed in Tables 1 and 2 against HSV-2 (*Herpesviridae*) versus vaccinia virus

(*Poxviridae*) in Vero cells forms a linear relationship (Figure 2). This linearity was maintained when comparing IC<sub>50</sub>s for inhibition of HSV-2 with other susceptible viruses, including MHV, Modoc, and Rhino viruses (see Supporting Information). The relationships did not achieve significance when comparing activity against HSV-2 with members of the *Bunyaviridae* (California Encephalitis and San Angelo viruses), although a tendency for a positive relationship is evident. These results suggest that in general 2-PB and 2-PIP compounds inhibit IgE and virus through a common mechanism.

Nonetheless, there is a decided potency advantage for IgE inhibition (Tables 1 and 2), although the difference appears to be less obvious for the 2-PIP compounds than the 2-PB derivatives. This is illustrated by directly comparing the relative potencies of matching 2-PB and 2-PIP compounds against IgE and virus; i.e., **2d** versus **4a**, **2a** versus **4b**, and **1d** versus **3c**. Expression of this relationship by averaging the IC<sub>50</sub>s of the

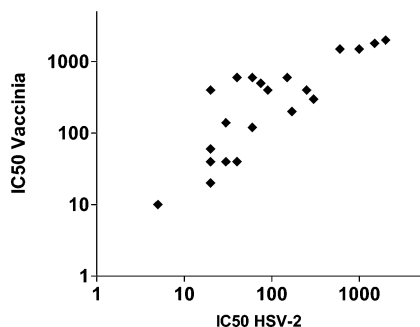


**Figure 2.** The  $IC_{50}$ s of all 24 compounds listed in Tables 1 and 2 against the propagation of HSV-2 and vaccinia virus are compared. Two-tailed comparison reveals a highly significant correlation between the inhibitory effects on the two viruses ( $P < 0.0001$ ).

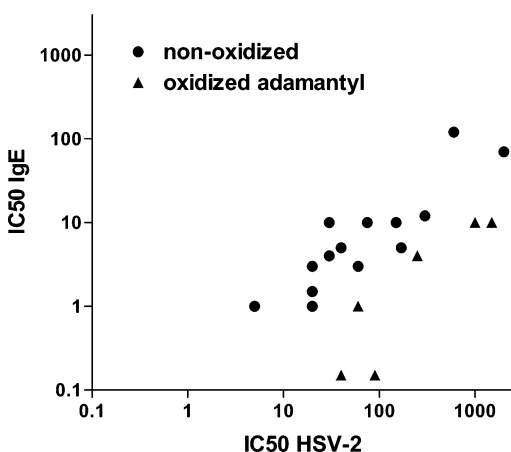


**Figure 3.** The  $IC_{50}$ s in Tables 1 and 2 for the suppression of IgE and HSV-2 are compared. Compounds with oxygen-substituted adamantyl groups are shown separately as triangles. Low potency compounds ( $IC_{50} > 2000$  nM) were omitted from the graph. 2-Tailed comparisons of IgE versus HSV-2 for all compounds in Tables 1 and 2 show a significant correlation ( $P = 0.0373$ ). When the same statistics are applied to the triangles and circles separately, each comparison resulted in  $P$  values of less than 0.0001. Similar comparisons between the  $IC_{50}$ s of all compounds versus IgE and susceptible viruses showed positive trends: vaccinia,  $P = 0.019$ ; MHV, 0.0087; California Encephalitis,  $P = 0.565$ ; San Angelo,  $P = 0.404$ ; Modoc,  $P = 0.0319$ ; and Rhino,  $P = 0.0065$ . In contrast, similar comparisons for SV40 and VSV growth did not yield significant correlations ( $P > 0.05$ ).

six compounds against all viruses (except VSV and SV40) in Tables 1 and 2 and dividing this hybrid figure by their  $IC_{50}$  against IgE yields a ratio of 23 for 2-PB compounds (**2d**, **2a**, **1d**) versus 4 for the corresponding 2-PIP derivatives (**4a**, **4b**, **3c**). While this comparison is based on only three pairs of compounds, it does suggest that the 2-PIP derivatives have stronger activity against virus than the 2-PB compounds.

Although the relationship between IgE and virus inhibition generally follows a linear pattern for all compounds, a few notable outliers are noted in Figure 3. This was first observed in the Table 1 compounds **1b** and **1e**, which have oxidized terminal adamantyl groups. Both compounds are over 100-fold more potent against IgE than HSV or vaccinia, whereas the parent compound (**1d**) shows only a 25-fold preference against IgE. Thus in selecting 2-PIP analogues for testing against virus, several with oxidized adamantyl groups were chosen (Table 2). As shown for the 2-PB derivatives, 2-PIP compounds containing oxygen on the terminal cyclic moieties (**4f**, **4d**, **4g**, **3b**) were considerably less potent for inhibiting virus relative to IgE, thus confirming the negative impact of oxygen substitution. The

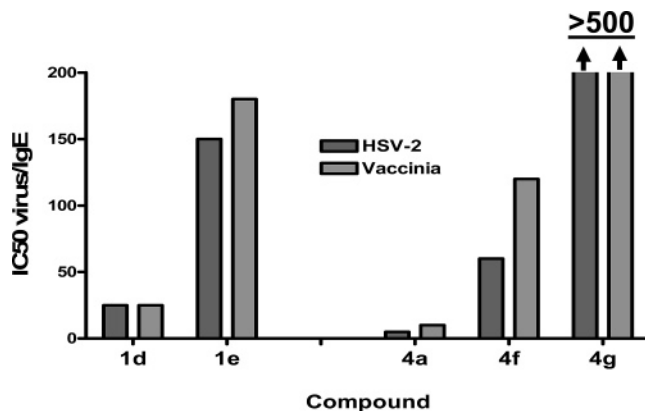


**Figure 4.** The effect of hydroxyl substitution on the terminal ring adamantyl. The anti-IgE and antiviral activity of compounds with terminal adamantyl groups, with and without hydroxyl substitutions, are compared. For each, a ratio of the  $IC_{50}$  for virus (HSV-2 or vaccinia virus) divided by the  $IC_{50}$  for IgE is plotted. The 2-PB compound **1d** is paired with its 4-OH-1-adamantyl analogue **1e**, and the 2-PIP compound **4a** is paired with its (phenyl side) 4-OH-1-adamantyl analogue **4f** and the (imidazopyridine side) 4-OH-1-adamantyl analogue **4g**.

potency for inhibition of IgE and virus is directly compared for compounds that differ only by the presence of oxygen moieties in the terminal adamantyl (Figure 4). For example, the  $IC_{50}$  ratio for IgE/virus for **1d** is 25 while for **1e** the value rises to 150. Similar results were noted for 2-PIP compounds wherein the discrepancy between IgE and virus climbed from an average ratio of 8 for the unoxidized bisadamantyl compound (**4a**) to 90 with a 4-substituted OH on the right adamantyl (**4f**) and 1700 for the 4-substituted OH on the left adamantyl (**4g**). While the reason for the lower relative potency of these oxidized analogues is unknown, these more hydrophilic analogues have been shown to accumulate in lower relative intracellular concentrations than their nonoxidized forms (data not shown). Although this would suggest that reduced cellular penetration or retention of the oxidized analogues may translate to a reduced effect on virus, why the same effect is not observed for IgE responses is not known.

To demonstrate that the antiviral activity can translate to an in vivo model, selected compounds were tested in a topical model of HSV infection, including the compound currently in clinical trials for asthma and allergy (**1d**) and the highly potent 2-PIP compound **4a**. A topical approach obviates other potential in vivo effects of these agents such as on cytokines, thus simplifying interpretation of the results. This is all the more important because of the lower potency and thus higher anticipated dosing required for suppression of virus than IgE or cytokines. Guinea pigs were infected with HSV-2 and treatment initiated the following day with drug (2%) or vehicle four times a day for 3 days. The efficacy of **1d** was no better than vehicle (data not shown); representative results for **4a** are illustrated in Figure 5. While a modest effect was noted for vehicle, an ointment containing 2% **4a** completely suppressed the appearance of vesicles. We are unaware of previous reports illustrating this level of response. The difference in response between **1d** and **4a** can be explained by lipid solubility and potency, both of which favor **4a**. Lipid solubility would translate to improved skin penetration. Moreover, based on a 300-fold potency advantage for **4a** and an  $ED_{50}$  of 0.5% (data not shown), a concentration of 30% of **1d** would be minimally required to achieve efficacy. These results underscore the potential utility of **4a** for treating viral infections, at least in topical applications.



**Figure 5.** Prevention of HSV-2 vesicle formation in a guinea pig model of topical herpes. HSV-2 (MS strain) was inoculated on the back of six hairless guinea pigs in three distinct sites such that each guinea pig served as its own control. Treatment sites were rotated. Topical treatment was initiated on day 2 with 100  $\mu$ L of vehicle, 100  $\mu$ L of 2% **4a**, or nothing, and repeated four times a day for 3 days. The guinea pigs were photographed each day until maximum viral response could be assessed, which occurred on day 4. Shown are representative responses from each treatment group.

## Conclusion

This report describes the antiviral activity of a group of 2-(substituted phenyl)benzimidazole compounds (series **1** and **2**), as well as the synthesis and antiviral activity of a novel group of imidazopyridine (series **3** and **4**) derivatives. Viruses inhibited by these compounds comprise several families that are important causes of human disease and which rely on the Golgi for their envelopment and processing. While the antiviral activity of most of the compounds parallels their anti-IgE activity, those with oxidized terminal adamantyl groups substantially lose antiviral potency without affecting their inhibition of IgE. The imidazopyridine derivatives are more potent than the benzimidazoles against virus, and one of the former agents **4a** is highly effective in a guinea pig model of herpes infection. These results support further investigation of these compounds for the treatment of many viral pathogens.

## Experimental Section

**Compounds 3a–e. 4-Aminopyridine-2-carboxylic Acid.** The picloram methyl ester (55.0 g, 0.215 mmol) was dissolved in 10% LiOH (0.3 L), and then 8.0 g 10% palladium carbon (wet) was added

carefully. The mixture was shaken in Parr shaker 4 h at 40 °C and then overnight at 70 °C. The catalyst was removed by filtration, and the solution was adjusted to pH 3 with concd HCl (approximately 20 mL). The product immediately precipitated, and the reaction mixture was left at 4 °C for 3 h. Filtration, washing with minimal volume of ice–water, and drying over vacuum gave 22.4 g (77%) of 4-aminopyridine-2-carboxylic acid as a fine off-white solid.

**Ethyl 4-Amino-5-nitropyridine-2-carboxylate.** Potassium nitrate (6.2 g, 61.3 mmol) was added to a cooled solution of 4 aminopyridine-2-carboxylic acid (8.46 g, 61.3 mmol) in concd H<sub>2</sub>SO<sub>4</sub> (60 mL). After being stirred 20 min at room temperature, the reaction mixture was heated at 75 °C for 2 h. The reaction mixture was again cooled to 0 °C in an ice bath, and 180 mL of ice cold ethanol was added with stirring. The resulting mixture was stirred at 60 °C overnight and then cooled to room temperature. The reaction mixture was slowly added to an ice cold potassium acetate solution (240 g in 0.450 L of water) resulting in the precipitation of product mixed with potassium sulfate. The product was filtered and washed several times with ice cold water yielding 8.74 g (68%) of ethyl 4-amino-5-nitropyridine-2-carboxylate as an off-white colored solid. <sup>1</sup>H NMR (400 MHz, DMSO-*d*<sub>6</sub>):  $\delta$  14.0 (1H, br s, NH<sub>2</sub>), 9.0 (1H, s, Ar–H), 8.20 (1H, br s, NH), 6.66 (1H, s, Ar–H), 4.36 (1H, q, *J* = 6.0 Hz, CH<sub>2</sub>–CH<sub>3</sub>), 1.30 (3H, t, *J* = 6.0 Hz, CH<sub>2</sub>–CH<sub>3</sub>).

**Ethyl 4,5-Diaminopyridine-2-carboxylate (5).** Ethyl 4-amino-5-nitropyridine-2-carboxylate (13.3 g, 63.0 mmol) was reduced with 10% Pd/C (2.60 g) in a cyclohexene/2-propanol mixture (15 mL/100 mL) under reflux conditions for 12 h. The reaction mixture was freed from catalyst, and solvent was evaporated to afford ethyl 4,5-diaminopyridine-2-carboxylate (**5**, 11.3 g, 99%). <sup>1</sup>H NMR (400 MHz, DMSO-*d*<sub>6</sub>):  $\delta$  7.70 (1H, s, Ar–H), 7.21 (1H, s, Ar–H), 5.51 (2H, br s, NH<sub>2</sub>), 5.25 (2H, br s, NH<sub>2</sub>), 4.20 (2H, q, *J* = 6.0 Hz, CH<sub>2</sub>–CH<sub>3</sub>), 1.26 (3H, t, *J* = 6.0 Hz, CH<sub>2</sub>–CH<sub>3</sub>); MS *m/z*: 182.1 (M + H<sup>+</sup>).

**Ethyl 2-(4-Nitrophenyl)-3H-imidazo[4,5-*c*]pyridine-6-carboxylate (7):** Ethyl 4,5 diaminopyridine-2-carboxylate (**5**, 10.86 g, 60.0 mmol) and 4-nitrobenzaldehyde (**6**, 11.0 g, 1.2 equiv) were refluxed in nitrobenzene (100 mL) at 200 °C for 18 h. The reaction mixture was cooled and diluted with diethyl ether (1 L), and the solid was filtered. The solid was washed with additional volumes of ether and dried in vacuum (**7**, 15.9 g, 83%). <sup>1</sup>H NMR (400 MHz, DMSO-*d*<sub>6</sub>):  $\delta$  13.65 (1H, br s, NH), 9.09 (1H, s, Ar–H), 8.47 (1H, 4H, m, Ar–H), 8.33 (1H, br s, Ar–H), 4.35 (1H, q, *J* = 6.0 Hz, CH<sub>2</sub>–CH<sub>3</sub>), 1.35 (3H, t, *J* = 6.0 Hz, CH<sub>2</sub>–CH<sub>3</sub>); MS *m/z*: 285 (M + H<sup>+</sup>).

**2-(4-Nitrophenyl)-3H-imidazo[4,5-*c*]pyridine-6-carboxylic Acid (8).** The ester **7** (9.75 g, 31.25 mmol) was dissolved in 10% NaOH (80 mL) and EtOH (200 mL) and refluxed at 90 °C for 1 h. The reaction mixture was filtered and acidified with 3 N HCl (100 mL), and a reddish brown solid was filtered, washed with H<sub>2</sub>O and methanol, and dried under high vacuum yielding **8** (8.24 g, 93%). <sup>1</sup>H NMR (400 MHz, DMSO-*d*<sub>6</sub>):  $\delta$  14.00 (1H, br s, CO<sub>2</sub>H), 8.91 (1H, br s, Ar–H), 8.56 (2H, br m, Ar–H), 8.41 (2H, br m, Ar–H), 8.25 (1H, br s, Ar–H).

**N-Adamantyl-2-(4-nitrophenyl)-3H-imidazo[4,5-*c*]pyridine-6-carboxamide (9a).** CDI (0.255 g, 1.5 equiv) was added to a solution of acid **8** (0.300 g, 1.05 mmol) in dry DMF (10 mL) and heated at 80 °C for 3 h. Two batches of adamantinamine (0.226 g, 1.5 mmol) were added at 2 h interval, and the reaction mixture was heated at 100 °C for 16 h. The mixture was poured into water, and a yellow solid **9a** was filtered (0.210 g, 50%). MS *m/z*: 418 (M + H<sup>+</sup>). The solid was used for the next step without further purification.

**N-(4-Oxadamantyl)-2-(4-nitrophenyl)-3H-imidazo[4,5-*c*]pyridine-6-carboxamide (9b).** The nitro acid **8** (0.215 g, 0.76 mmol) was stirred with PyBop (0.600 g, 1.5 equiv) in DMF (5 mL) at room temperature for 16 h. 4-Oxadamantamine hydrochloride salt (0.230 g, 1.15 mmol), DMAP (0.080 g, 0.76 mmol), and pyridine (20 mL) were added and stirred overnight. The reaction mixture

was poured into water and the solid was filtered (**9b**, 0.300 g, 90%) and used for the next step.

**2-(4-Nitrophenyl)-N-(pyridin-2-yl)-3H-imidazo[4,5-c]pyridine-6-carboxamide (9c).** This compound was prepared by using a similar method as described for **9a** using **8** (1.0 g, 3.5 mmol) and 2-aminopyridine (0.5 g, 5.3 mmol). Following filtration, a yellow solid was obtained (**9c**, 0.850 g, 66%) and used for the next step without further purification.

**2-(4-Aminophenyl)-N-(adamantyl)-3H-imidazo[4,5-c]pyridine-6-carboxamide (10a).** A solution of **9a** (0.210 g, 0.50 mmol) was reduced with Raney nickel (0.300 mL) in a mixture of MeOH/THF (15 mL/5 mL) at 85 °C for 2 h under H<sub>2</sub> atmosphere. The product was freed from catalyst and evaporated to dryness (**10a**, 0.190 g, 98%). The amine **10a** was used for the next step without further purification.

**2-(4-Aminophenyl)-N-(4-oxoadamantyl)-3H-imidazo[4,5-c]pyridine-6-carboxamide (10b).** The nitroamide **9b** (0.200 g, 0.46 mmol) was stirred with 10% palladium on carbon (0.050 g) in EtOH-THF (3:1) mixture at room temperature for 16 h. The amine was freed from catalyst, and the solvent was evaporated to yield **10b** (0.100 g, 97%), which was used for the next step without further purification.

**2-(4-Aminophenyl)-N-(pyridin-2-yl)-3H-imidazo[4,5-c]pyridine-6-carboxamide (10c).** The nitropyridine amide **9c** (0.458 g, 1.27 mmol) was reduced over 10% palladium carbon (0.100 g) in MeOH-THF-DMF mixture (10 mL-10 mL-2.5 mL) at 80 °C for 7 h. The amine amide was freed from catalyst and solvent was removed. Water was added, and yellow solid was filtered (**10c**, 0.178 g, 40%) and used for the next step.

**2-(4-(Adamantanecarboxamido)phenyl)-N-(pyridin-2-yl)-3H-imidazo[4,5-c]pyridine-6-carboxamide (3c).** Adamantine carbonyl chloride (0.208 g, 1.04 mmol) was added to a solution of amine **10c** (0.230 g, 0.69 mmol) in pyridine (5 mL), and the reaction mixture was further stirred at room temperature for 16 h. The reaction was quenched with water and solid was filtered. The solid was dissolved in MeOH-EtOAc and reprecipitated with ether yielding **3c** (0.148 g, 43%). Mp 356 °C; <sup>1</sup>H NMR (400 MHz, DMSO-*d*<sub>6</sub>): δ 13.64 (1H, br s, NH), 10.54 (1H, s, NH), 9.38 (1H, s, NH), 8.95 (1H, m, Ar-H), 8.45 (2H, d, *J* = 7.6 Hz, Ar-H), 8.28 (2H, d, *J* = 8.4 Hz, Ar-H), 7.88 (3H, m, Ar-H), 7.15 (1H, m, Ar-H), 2.70 (3H, br s, adamantyl), 1.73 (6H, br s, adamantyl), 1.39 (6H, br s, adamantyl); MS *m/z*: 493.6 (M<sup>+</sup>); Anal. (C<sub>29</sub>H<sub>28</sub>N<sub>6</sub>O<sub>8</sub>·H<sub>2</sub>O) C, H, N, S.

Compounds **3a**, **3b**, and **3d** were prepared by applying a method similar to that described for **3c**.

**2-(4-(4-Chlorophenylamido)phenyl)-N-adamantyl-3H-imidazo[4,5-c]pyridine-6-carboxamide (3a).** Mp 364 °C; <sup>1</sup>H NMR (400 MHz, DMSO-*d*<sub>6</sub>): δ 13.45 (1H, br s, NH), 10.48 (1H, s, NH), 9.43 (1H, s, NH), 8.96 (1H, m, Ar-H), 8.24 (7H, m, Ar-H), 7.61 (2H, m, Ar-H), 2.12 (9H, m, adamantyl), 1.62 (6H, m, adamantyl); MS *m/z*: 526.4 (M<sup>+</sup>); Anal. (C<sub>30</sub>H<sub>28</sub>ClN<sub>5</sub>O<sub>2</sub>·H<sub>2</sub>O) C, H, N, S.

**N-(4-Chlorophenyl)-2-(4-(4-oxoadamantanecarboxamido)phenyl)-3H-imidazo[4,5-c]pyridine-6-carboxamide (3b).** Mp 343 °C; <sup>1</sup>H NMR (400 MHz, DMSO-*d*<sub>6</sub>): δ 13.55 (1H, br s, NH), 10.59 (1H, s, NH), 9.43 (1H, s, NH), 8.97 (1H, m, Ar-H), 8.14 (7H, m, Ar-H), 7.63 (2H, m, Ar-H), 2.65-1.80 (13H, m, adamantyl); MS *m/z*: 540.5 (M<sup>+</sup>); Anal. (C<sub>30</sub>H<sub>26</sub>ClN<sub>5</sub>O<sub>3</sub>·H<sub>2</sub>O) C, H, N, S.

**2-(4-(3-Hydroxyadamantanecarboxamido)phenyl)-N-(4-oxoadamantane)-3H-imidazo[4,5-c]pyridine-6-carboxamide (3d).** Mp 367 °C; <sup>1</sup>H NMR (400 MHz, DMSO-*d*<sub>6</sub>): δ 13.59 (1H, br s, NH), 9.43 (1H, s, NH), 8.89 (1H, s, NH), 8.18 (4H, m, Ar-H), 7.93 (2H, m, Ar-H), 4.70 (1H, s, OH), 3.73-3.60 (1H, br s, 4Heq and 4Hax, 4-hydroxyadamantyl), 2.3-1.20 (26H, series of m, adamantyl); MS *m/z*: 580.5 (M<sup>+</sup>); Anal. (C<sub>34</sub>H<sub>37</sub>N<sub>5</sub>O<sub>4</sub>·2H<sub>2</sub>O) C, H, N, S.

**2-(4-(Adamantanecarboxamido)phenyl)-N-adamantyl-3H-imidazo[4,5-c]pyridine-6-carboxamide (3e).** The amine **10a** (0.190 g, 0.49 mmol) and adamantane carbonyl chloride (0.195 g, 2.0 mmol) were dissolved in pyridine (5 mL) and stirred at room temperature for overnight. The reaction mixture was poured into water, and solid **3e** was filtered and recrystallized with ethyl acetate (0.210 g, 80%). Mp 396 °C; <sup>1</sup>H NMR (400 MHz, DMSO-*d*<sub>6</sub>): δ

13.64 (1H, br s, NH), 9.57 (1H, s, NH), 9.38 (1H, s, NH), 9.02 (1H, s, Ar-H), 8.99 (1H, s, Ar-H), 8.18 (4H, m, Ar-H), 2.2-1.60 (30H, series of m, adamantyl); MS *m/z*: 550.6 (M<sup>+</sup>); Anal. (C<sub>34</sub>H<sub>39</sub>N<sub>5</sub>O<sub>2</sub>·H<sub>2</sub>O) C, H, N, S.

**Compounds 4a-g. tert-Butyl 2-(4-Nitrophenyl)-3H-imidazo[4,5-c]pyridin-6-ylcarbamate (11).** To a stirring solution of nitro acid **8** (10.7 g, 37.7 mmol) and triethylamine (5.8 mL, 1.1 equiv) in NMP (100 mL) was added diphenylphosphoryl azide (9.0 mL, 1.1 equiv) dropwise, and the reaction mixture was further stirred at room temperature overnight. Tertiary butanol (100 mL) was added, and the reaction mixture was heated at 85 °C for 6 h. After being cooled to room temperature, the reaction mixture was treated slowly with 100 mL of saturated NaHCO<sub>3</sub> followed by 200 mL water, heated to 85 °C for 10 min, and filtered hot. The filter cake was rinsed with additional water and dried in vacuum to get the yellow solid **11** (10.2 g, 76%). <sup>1</sup>H NMR (400 MHz, DMSO-*d*<sub>6</sub>): δ 13.86 (1H, br s, NH), 9.70 (1H, br s, NH), 8.72 (1H, br s, Ar-H), 8.47 (4H, br m, Ar-H), 7.99 (1H, br s, Ar-H), 1.51 (9H, s, Boc); MS *m/z*: 356.4 (M + H<sup>+</sup>).

**tert-Butyl 2-(4-aminophenyl)-3H-imidazo[4,5-c]pyridin-6-ylcarbamate (12).** The nitro carbamate **11** (10.2 g, 29.0 mmol) was dissolved in NMP (120 mL) and reduced over 10% Pd/C (2.0 g) in Parr shaker at 45 °C for 12 h. The amine carbamate **12** was freed from catalyst, and NMP was evaporated. To the residue was added THF, and solid was filtered. The THF layer was evaporated, affording the amine **12** (7.0 g, 70%). <sup>1</sup>H NMR (400 MHz, DMSO-*d*<sub>6</sub>): δ 12.74 (1H, br s, NH), 9.62 (1H, s, NH), 8.46 (1H, s, Ar-H), 7.95 (3H, m, Ar-H), 6.69 (2H, s, Ar-H), 5.70 (2H, s, NH<sub>2</sub>), 1.50 (9H, s, Boc); MS *m/z*: 326.4 (M + H<sup>+</sup>).

**2-(4-Aminophenyl)-3H-imidazo[4,5-c]pyridin-6-amine Dihydrochloride (13).** To a solution of amine carbamate **12** (1.0 g, 3.07 mmol) in dioxane (5 mL) was added 4 M HCl solution in dioxane (7 mL), and reaction mixture was heated at 90 °C for 1 h. The solid was filtered and washed with THF, affording the diamine salt **13** (0.83 g, 91%). <sup>1</sup>H NMR (400 MHz, DMSO-*d*<sub>6</sub>): δ 12.15 (1H, br s, NH), 8.20 (2H, s, Ar-H), 7.77 (2H, m, Ar-H), 6.78 (2H, s, Ar-H), 5.65 (4H, br s, NH<sub>2</sub>); MS *m/z*: 226 (M + H<sup>+</sup>).

**tert-Butyl 2-(4-(4-Oxoadamantanecarboxamido)phenyl)-3H-imidazo[4,5-c]pyridin-6-ylcarbamate (14d).** To a solution of **12** (0.305 g, 0.94 mmol) in dry pyridine (5 mL) was added 4-oxoadamantane carbonyl chloride (0.330 g, 1.55 mmol), and the reaction mixture was stirred at room temperature for 16 h. The crude **14d** was hydrolyzed with 4 M HCl (4 mL) in dioxane at 90 °C for 1 h, and amine salt was filtered (**14d**, 0.340 g, 84% in two steps).

**tert-Butyl 2-(4-(adamantanecarboxamido)phenyl)-3H-imidazo[4,5-c]pyridin-6-ylcarbamate (14e).** A solution of aminocarbamate **12** (0.325 g, 1.0 mmol), adamantane carbonyl chloride (0.300 g, 1.5 mmol) in pyridine (5 mL) was stirred at room temperature for overnight yielding crude **14e** (0.460 g). The crude **14e** (0.465 g, 0.94 mmol) was dissolved in 4.0 M HCl in dioxane (5 mL) and stirred at 90 °C for 1 h. The amine salt was filtered (**14e**, 0.270 g, 64% in two steps).

**N-(4-(6-(Adamantanecarboxamido)-3H-imidazo[4,5-c]pyridin-2-yl)phenyl)adamantanecarboxamide (4a).** To a solution of diamine hydrochloride **13** (0.200 g, 0.50 mmol) in dry pyridine (10 mL) was added adamantane carbonyl chloride (0.250 g, 0.150 mmol), and the reaction mixture was heated at 120 °C for 3 h. The reaction mixture was added to water, and solid was filtered. The solid was stirred with 10% NaOH (3 mL) in EtOH (10 mL) at room temperature for 1 h. The EtOH was evaporated, water was added, and the solid was filtered. The off white solid was passed through a short bed of SiO<sub>2</sub> gel using THF as a solvent. The solvent was evaporated, and solid was crystallized from MeOH to yield **4a** (0.150 g, 50%). Mp 265 °C; <sup>1</sup>H NMR (400 MHz, DMSO-*d*<sub>6</sub>): δ 13.02 (1H, br s, NH), 9.48 (1H, br s, NH), 9.37 (1H, br s, NH), 8.64 (1H, s, Ar-H), 8.24 (1H, s, Ar-H), 8.08 (2H, d, *J* = 5.0 Hz, Ar-H), 7.88 (2H, d, *J* = 5.0 Hz, Ar-H), 2.03-1.60 (30 H, series of m, adamantyl); MS *m/z*: 449.6 (M + H<sup>+</sup>); Anal. (C<sub>34</sub>H<sub>39</sub>N<sub>5</sub>O<sub>2</sub> × 0.85H<sub>2</sub>O) C, H, N.

**N-(4-(6-(Cyclohexanecarboxamido)-3H-imidazo[4,5-c]pyridin-2-yl)phenyl)cyclohexanecarboxamide (4b).** A solution of **13**



(0.080 g, 0.24 mmol) in dry pyridine (10 mL) and cyclohexanecarbonyl chloride (0.120 mL, 0.76 mmol) was heated at 100 °C for 3 h. The reaction mixture was quenched with water, gummy solid was filtered, and the filtrate was stirred with 10% NaOH (2 mL) in EtOH (10 mL) at room temperature for 1 h. The solvent was evaporated, water was added, and solid was filtered. The solid was passed through a bed of SiO<sub>2</sub> gel. Elution with ethyl acetate afforded **4b** as light yellow solid (0.055 g, 51%). Mp 235 °C; <sup>1</sup>H NMR (400 MHz, DMSO-*d*<sub>6</sub>): δ 12.99 (1H, br s, NH), 10.27 (1H, br s, NH), 10.07 (1H, br s, NH), 8.61 (1H, br s, Ar-H), 8.27 (1H, br s, Ar-H), 8.07 (2H, d, *J* = 8.0 Hz, Ar-H), 7.79 (2H, d, *J* = 9.0 Hz, Ar-H), 2.52 (1H, m, cyclohexyl), 2.36 (1H, m, cyclohexyl), 1.83–1.17 (20 H, series of m, cyclohexyl); MS *m/z*: 446.5 (M + H<sup>+</sup>), 444.6 (M - H<sup>+</sup>); Anal. (C<sub>26</sub>H<sub>31</sub>N<sub>5</sub>O<sub>2</sub> × 0.91H<sub>2</sub>O) C, H, N.

**N-(2-(4-(4-Oxadamantanecarboxamido)-3H-imidazo[4,5-c]pyridin-2-yl)phenyl)-4-oxadamantanecarboxamide (4c)**. To a solution of **13** (0.212 g, 0.71 mmol) in dry pyridine (10 mL) was added 4-ketoadamantanecarbonyl chloride (0.600 g, 4 equiv), and the reaction mixture was heated at 120 °C for 3 h. This afforded **4c** as an off-white solid (0.136 g, 30%). Mp 258–268 °C; <sup>1</sup>H NMR (400 MHz, DMSO-*d*<sub>6</sub>): δ 13.01 (1H, s, NH), 9.88 (1H, s, NH), 9.57 (1H, s, NH), 8.65 (1H, s, Ar-H), 8.22 (1H, s, Ar-H), 8.10 (2H, br d, *J* = 10.0 Hz, Ar-H), 7.86 (2H, br d, *J* = 10.0 Hz, Ar-H), 2.47 (2H, br m, adamantyl), 2.32 (2H, br m, adamantyl), 2.24–2.15 (14H, m, adamantyl), 2.06 (4H, br m, adamantyl), 1.89 (4H, br m, adamantyl); MS *m/z*: 578.8 (M<sup>+</sup>); Anal. (C<sub>34</sub>H<sub>35</sub>N<sub>5</sub>O<sub>4</sub> × 1 H<sub>2</sub>O) C, H, N, S.

**N-(2-(4-(4-Oxadamantanecarboxamido)phenyl)-3H-imidazo[4,5-c]pyridin-6-yl)adamantanecarboxamide (4d)**. To a solution of amine **14** (0.160 g, 0.40 mmol) in dry pyridine (10 mL) was added adamantane carbonyl chloride (0.120 g, 0.42 mmol), and the reaction mixture was stirred at 120 °C for 4 h. After the usual workup, this afforded the desired product **4d** (0.080 g, 35%). Mp 250 °C; <sup>1</sup>H NMR (400 MHz, DMSO-*d*<sub>6</sub>): δ 13.05 (1H, br s, NH), 9.56 (1H, br s, NH), 9.46 (1H, br s, NH), 8.26 (1H, br s, Ar-H), 8.24 (1H, br s, Ar-H), 8.11 (2H, d, *J* = 10.0 Hz, Ar-H), 7.87 (2H, d, *J* = 10.0 Hz, Ar-H), 2.47 (1H, br m, adamantyl), 2.32 (1H, br m, adamantyl), 2.20–1.80 (26H, br m and br s, adamantyl); MS *m/z*: 564 (M + H<sup>+</sup>); Anal. (C<sub>34</sub>H<sub>37</sub>N<sub>5</sub>O<sub>3</sub> × 1.36H<sub>2</sub>O).

**N-(2-(4-(Adamantanecarboxamido)phenyl)-3H-imidazo[4,5-c]pyridin-6-yl)pyridine-2-carboxamide (4e)**. A solution of amine **14** (0.065 g, 0.197 mmol) and adamantane carbonyl chloride (0.060 g, 0.30 mmol) in dry pyridine (5 mL) was stirred at 80 °C for 2 h. The resulting solid was treated with 10% NaOH for 1 h. The solid was filtered and passed through SiO<sub>2</sub> gel. Elution with EtOAc afforded diamide **4e** (0.039 g, 40%). Mp 305 °C; <sup>1</sup>H NMR (400 MHz, DMSO-*d*<sub>6</sub>): δ 13.19 (1H, br s, NH), 10.47 (1H, br s, NH), 9.39 (1H, br s, NH), 8.76 (1H, d, *J* = 4.5 Hz, Ar-H), 8.73 (1H, br s, Ar-H), 8.45 (1H, br s, Ar-H), 8.24 (1H, d, *J* = 8.0 Hz, Ar-H), 8.11 (3H, m, Ar-H), 7.89 (2H, d, *J* = 8.5 Hz, Ar-H), 7.72 (1H, dt, *J* = 5.0 and 7.5 Hz, Ar-H), 2.0 (3H, br s, adamantyl), 1.92 (6H, br s, adamantyl), 1.72 (6H, br s, adamantyl); MS *m/z*: 493.5 (M + H<sup>+</sup>); Anal. (C<sub>29</sub>H<sub>28</sub>N<sub>6</sub>O<sub>2</sub> × 1.23H<sub>2</sub>O) C, H, N.

**N-(2-(6-(Adamantanecarboxamido)-3H-imidazo[4,5-c]pyridin-2-yl)phenyl)-4-hydroxyadamantanecarboxamide (4f)**. To a solution of **4d** (0.080 g, 0.142 mmol) in EtOH (10 mL) was added NaBH<sub>4</sub> (0.038 g, 1.0 mmol), and the reaction mixture was stirred at 90 °C for 1 h. Ethanol was removed, and the residue was washed with water. The product was dissolved in MeOH and THF and filtered to remove inorganic residue. The product **4f** was precipitated with MeOH–EtOAc as a white solid and filtered (0.035 g, 43%). <sup>1</sup>H NMR (400 MHz, DMSO-*d*<sub>6</sub>): δ 13.05 (1H, br s, NH), 9.36 (2H, br s, NH), 8.59 (1H, br s, Ar-H), 8.29 (1H, br s, Ar-H), 8.10 (2H, d, *J* = 8.3 Hz, Ar-H), 7.85 (2H, br d, *J* = 8.3 Hz, Ar-H), 4.70 (1H, br s, OH), 3.72–3.60 (1H, br s, 4Heq and 4Hax of 4-hydroxyadamantyl), 2.20–1.40 (28H, series of m, adamantyl); MS *m/z*: 566.6 (M + H<sup>+</sup>), 601.5 (M + Cl<sup>-</sup>); Anal. (C<sub>34</sub>H<sub>39</sub>N<sub>5</sub>O<sub>3</sub> × 3.5H<sub>2</sub>O) C, H, N.

**N-(2-(4-(Adamantanecarboxamido)phenyl)-3H-imidazo[4,5-c]pyridin-6-yl)-4-hydroxyadamantanecarboxamide (4g)**. This compound was made similar to **4f**. Mp 356 °C; <sup>1</sup>H NMR (400 MHz, DMSO-

*d*<sub>6</sub>): δ 9.35 (2H, m, NH<sub>2</sub>), 8.50 (1H, s, Ar-H), 8.20 (1H, s, Ar-H), 8.10 (2H, m, Ar-H), 7.85 (2H, m, Ar-H), 4.70 (1H, br s, OH), 3.72–3.60 (1H, br s, 4Heq and 4Hax of 4-hydroxyadamantyl), 2.30–1.30 (28H, series of m, adamantyl); MS *m/z*: 601.5 (M<sup>+</sup>); Anal. (C<sub>34</sub>H<sub>39</sub>N<sub>5</sub>O<sub>3</sub> × 3H<sub>2</sub>O) C, H, N, S.

**Acknowledgment.** The authors thank Dr. Sunil Kumar KC for critical review of the manuscript.

**Supporting Information Available:** Experimental procedures and spectral data. This material is available via the Internet at <http://pubs.acs.org>.

## References

- (1) (a) Grant, R. M.; Hecht, F. M.; Warmerdam, M.; Liu, L.; Liegler, T.; Petropoulos, C. J.; Hellman, N. S.; Chesney, M.; Busch, M. P.; Kahn, J. O. Time trends in primary HIV-1 drug resistance among recently infected persons. *JAMA* **2002**, *288*, 181–188. (b) Iannello, A.; Debbeche, O.; Martin, E.; Attalah, L. H.; Samarani, S.; Ahmad, A. Viral strategies for evading antiviral cellular immune responses of the host. *J. Leukoc. Biol.* **2006**, *79*, 16–35.
- (2) Lippincott-Schwartz, J.; Yuan, L. C.; Bonifacino, J. S.; Klausner, R. D. Rapid redistribution of Golgi proteins into the ER in cells treated with brefeldin A: evidence for membrane cycling from Golgi to ER. *Cell* **1989**, *56*, 801–813.
- (3) Richards, M. L.; Lio, S. C.; Sinha, A.; Tieu, K. K.; Sircar, J. C. Novel 2-(substituted phenyl)benzimidazole derivatives with potent activity against IgE, cytokines, and CD23 for the treatment of allergy and asthma. *J. Med. Chem.* **2004**, *47*, 6451–6454.
- (4) Richards, M. L.; Lio, S. C.; Sinha, A.; Banie, H.; Thomas, R. J.; Major, M.; Tanji, M.; Sircar, J. Substituted 2-phenyl-benzimidazole derivatives: novel compounds that suppress key markers of allergy. *Eur. J. Med. Chem.* **2006**, *41*, 950–969.
- (5) Lio, S. C.; Johnson, J.; Chatterjee, A.; Ludwig, J. W.; Millis, D.; Banie, H.; Sircar, J. C.; Sinha, A.; Richards, M. L. Disruption of Golgi processing by 2-(substituted phenyl) benzimidazole derivatives blocks cell proliferation and slows tumor growth. *Cancer Chemother. Pharmacol.* **2007**, in press. Epub ahead of print.
- (6) Ludwig, J. W.; Richards, M. L. Targeting the secretory pathway for anti-inflammatory drug development. *Curr. Top. Med. Chem.* **2006**, *6*, 165–178.
- (7) (a) Ludwig, J. W.; Soneff, R.-M.; Banie, H.; Marcantonio, D.; Scholz, W.; Galang, C.; Johnson, J.; Sircar, J. C.; Chatterjee, A.; Richards, M. L. Novel 2-phenyl-benzimidazole inhibitors of cytokines and cellular proliferation foster Golgi enzyme depletion through accelerated degradation. *Eur. J. Pharmacol.* **2007** (submitted for publication). (b) Ludwig, J. W.; Banie, H.; Galang, C.; Lio, S. C.; Sircar, J. C.; Richards, M. L. Golgi processing defect induced by AVP-13358 results in a loss of processing and expression of CD23. **2007** (Manuscript in preparation).
- (8) Marcelletti, J. F.; Katz, D. H. Elicitation of antigen-induced primary and secondary murine IgE antibody responses in vitro. *Cell. Immunol.* **1991**, *135*, 471–489.
- (9) (a) Beznoussenko, G. V.; Mironov, A. A. Models of intracellular transport and evolution of the Golgi complex. *Anat. Rec.* **2002**, *268*, 226–238. (b) Pelham, H. R.; Rothman, J. E. The debate about transport in the Golgi—two sides of the same coin? *Cell* **2000**, *102*, 713–719. (c) Marsh, B. J.; Howell, K. E. The mammalian Golgi—complex debates. *Nat. Rev. Mol. Cell Biol.* **2002**, *3*, 789–795. (d) Storrie, B.; Pepperkok, R.; Nilsson, T. Breaking the COPI monopoly on Golgi recycling. *Trends Cell Biol.* **2000**, *10*, 385–391.
- (10) (a) Granzow, H.; Klupp, B. G.; Fuchs, W.; Veits, J.; Osterrieder, N.; Mettenleiter, T. C. Egress of alpha herpes viruses: comparative ultrastructural study. *J. Virol.* **2001**, *75*, 3675–3684. (b) Husain, M.; Moss, B. Vaccinia virus F13L protein with a conserved phospholipase catalytic motif induces colocalization of the B5R envelope glycoprotein in post-Golgi vesicles. *J. Virol.* **2001**, *75*, 7528–7542. (c) Pettersson, R. F.; Melin, L. Synthesis, assembly and intracellular transport of *Bunyaviridae* membrane proteins. In *The Bunyaviridae*; Elliott, R. M., Ed.; Springer-Verlag: Berlin, Germany, 1996; pp 159–188. (d) Gerrard, S. R.; Nichol, S. T. Characterization of the Golgi retention motif of Rift Valley fever virus (G) glycoprotein. *J. Virol.* **2002**, *76*, 12200–12210. (e) Klumperman, J.; Locker, J. K.; Meijer, A.; Horzinek, M. C.; Geuze, H. J.; Rottier, P. J. Coronavirus M proteins accumulate in the Golgi complex beyond the site of viron budding. *J. Virol.* **1994**, *68*, 6523–6534. (f) Mackenzie, J. M.; Jones, M. K.; Westaway, E. G. Markers for trans-Golgi membranes and the intermediate compartment localize to induced membranes with distinct replication functions in flavivirus-infected cells. *J. Virol.* **1999**, *73*, 9555–9567.

- (11) de Jong, A. S.; Visch, H. J.; de Mattia, F.; van Dommelen, M. M.; Swarts, H. G.; Luyten, T.; Callewaert, G.; Melchers, W. J.; Willems, P. H.; van Kuppeveld, F. J. The coxsackievirus 2B protein increases efflux of ions from the endoplasmic reticulum and Golgi, thereby inhibiting protein trafficking through the Golgi. *J. Biol. Chem.* **2006**, *281*, 14144–14150.
- (12) Whitt, M. A.; Zagouras, P.; Crise, B.; Rose, J. K. A fusion-defective mutant of the vesicular stomatitis virus glycoprotein. *J. Virol.* **1990**, *64*, 4907–4913.
- (13) Pelkmans, L.; Puntener, D.; Helenius, A. Local actin polymerization and dynamin recruitment in SV40-induced internalization of caveolae. *Science* **2002**, *296*, 535–539.
- (14) Norkin, L. C.; Anderson, H. A.; Wolfrom, S. A.; Oppenheim, A. Caveolar endocytosis of simian virus 40 is followed by brefeldin A-sensitive transport to the endoplasmic reticulum, where the virus disassembles. *J. Virol.* **2002**, *76*, 5156–5166.

JM0704907